Optical Fiber Technology xxx (2016) xxx–xxx

Contents lists available at ScienceDirect

Optical Fiber Technology

www.elsevier.com/locate/yofte

Invited Papers

Few-mode multicore fibers for long-haul transmission line

Yusuke Sasaki [a,*], Katsuhiro Takenaga [a], Shoichiro Matsuo [a], Kazuhiko Aikawa [a], Kunimasa Saitoh [b]

[a] *Fujikura Ltd., 1440, Mutsuzaki, Sakura, Chiba 285-8550, Japan*
[b] *Graduate School of Information Science and Technology, Hokkaido University, Sapporo 060-0814, Japan*

ARTICLE INFO

Article history:
Received 15 April 2016
Revised 12 August 2016
Accepted 29 September 2016
Available online xxxx

Keywords:
Optical fiber
Space-division multiplexing
Multicore fiber
Few-mode fiber
Few-mode multicore fiber

ABSTRACT

Few-mode multicore fibers (FM-MCFs) that enable dense space-division multiplexing (DSDM) have the potential to drastically improve the fiber capacity. In designing the FM-MCFs, several issues that originate from multicore fibers and few-mode fibers must be considered. In this paper, these design issues such as inter-core crosstalk (IC-XT) and dispersion mode delay (DMD) are discussed. A three-mode 12-core fiber with low-DMD low-IC-XT achieves long-haul DSDM transmission over 500 km. The design concept, fiber design, and characteristics of the fabricated three-mode 12-core fiber are also described.

1. Introduction

The transmission capacity of optical communication systems using single-mode fibers (SMFs) has been expanded in accordance with the increase of IP traffic. However, there is a limitation of capacity of approximately 100 Tbit/s owing to the fiber fuse phenomenon and Shannon limit [1]. Space-division multiplexing (SDM), realized by multicore fibers (MCFs) and few-mode fibers (FMFs), is expected to overcome the capacity limit of the current optical communication systems. An MCF has multiple cores in a single cladding. An FMF supports multiple transmission modes in a single core. Spatial channel count (SCC) [2] is expanded by using each core or mode of an MCF and an FMF as signal channels, respectively. The MCFs and FMFs have achieved several transmission records. The first transmission capacity over 1 Pbit/s [3] and capacity-distance product over 1 Ebit/s·km were achieved by 12-core SM-MCFs [4,5]. In addition, a 22-core SM-MCF has achieved the highest transmission capacity of 2.15 Pbit/s [6]. A single-core 10-mode fiber has achieved a transmission capacity of 115.2 Tbit/s [7]. However, it is predicted that further improvement in SCC and transmission characteristics will be difficult for the SM-MCFs or FMFs, because inter-core crosstalk (IC-XT) in an SM-MCF increases as the core count increases, and inter-LP-mode crosstalk (IM-XT) in an FMF increases as the mode count increases. These crosstalks also prevent the SDM from realizing long haul transmission. Thus, in order to realize future dense SDM (DSDM) systems, multicore fibers with few-mode cores, known as few-mode multicore fibers (FM-MCFs), are being investigated. The SCC of a fiber can be increased by using an FM-MCF, because the SCC of an FM-MCF is the core count multiplied by the mode count. SCC of over 100 was realized by FM-MCFs [8–10]. However, long-haul FM-MCF transmission over 500 km has only been achieved by a three-mode 12-core fiber with an SCC of 36 [11].

In this paper, we present the design and characteristics of our fabricated three-mode 12-core FM-MCF with a cladding diameter (D_c) of 230 μm, low dispersion mode delay (DMD) of less than |63| ps/km, and low IC-XT of less than −51.6 dB/500 km. First, general issues required for designing an FM-MCF are explained. This is followed by a review of many types of proposed FM-MCFs. Thirdly, techniques to fabricate the fiber are depicted, which include a heterogeneous core arrangement, arranging cores in a square lattice, and a graded index in the core profile. Finally, measured characteristics of the fabricated fiber are reported.

2. FM-MCF design issues

MCFs can be categorized into coupled MCFs and uncoupled MCFs. In the case of coupled MCFs, the transmission LP-modes in each core are strongly coupled among the cores, and supermodes are generated. DMD can be decreased by the use of supermodes. In contrast, uncoupled MCFs use the cores as independent waveguides to reduce the signal processing load. Reported FM-MCFs have been mainly based on uncoupled MCF technology. In designing these uncoupled FM-MCFs, the following issues relating

* Corresponding author.
E-mail address: yusuke.sasaki@jp.fujikura.com (Y. Sasaki).

http://dx.doi.org/10.1016/j.yofte.2016.09.017
1068-5200/© 2016 Published by Elsevier Inc.

to the MCFs and FMFs design must be addressed: (A) IC-XT, (B) core layout, (C) IM-XT, and (D) DMD.

Issue A is a common problem with SM-MCFs. Minimal IC-XT is preferable for long-haul transmission with multilevel modulation. For example, QPSK and 32QAM transmission with a Q-penalty of 0.5 dB require IC-XT values of less than −19 dB and −29 dB, respectively [3]. For SM-MCFs, IC-XT between the LP_{01} modes is the only IC-XT of concern. However, for FM-MCFs, we should also take into account the IC-XT relating to higher-order modes such as between the LP_{11} modes ($XT_{11\text{-}11}$) [12]. There is also IC-XT between different propagating modes such as between the LP_{11} mode and the LP_{01} mode ($XT_{11\text{-}01}$). Fig. 1 shows an example of the calculated core pitch dependencies of IC-XTs after 100 km propagation at 1550 nm and a bending diameter of 210 mm. Power coupling theory is used to calculate the IC-XT [13]. We assumed a core radius of 6.47 μm and a relative refractive index difference of 0.45% with a step index profile that supports LP_{01} and LP_{11} mode transmission over the C + L band (1530 nm–1625 nm) in practical use. The calculated effective areas (A_{eff}s) of the LP_{01} and the LP_{11} modes are 110 μm^2 and 170 μm^2 at 1550 nm, respectively. It is observed that $XT_{11\text{-}11}$ is larger than $XT_{01\text{-}01}$ by approximately 40 dB. This is because that higher-order mode has relatively large A_{eff} compared to that of the LP_{01} mode, and the confinement of higher-order modes is weaker than that of the fundamental mode. The $XT_{01\text{-}11}$ is also small because the difference in the effective indices between the LP_{01} and LP_{11} modes is large [14]. Thus, XT is dominated by $XT_{11\text{-}11}$ and therefore FM-MCFs should be designed with careful consideration of IC-XT related to the highest-order modes.

A common approach for reducing IC-XT is enlarging core pitch, which leads to a large D_c and deterioration of the mechanical reliability of a fiber. Reducing effective core area (A_{eff}) can also suppress IC-XT. However, reduced A_{eff} is inadequate for long-haul transmission systems owing to non-linear effects. In general, A_{eff} differs according to the propagation mode, and the A_{eff} of the LP_{01} mode is the smallest of all modes. It is desirable for the A_{eff} of the LP_{01} mode to be larger than that of conventional SMFs of around 80 μm^2 at 1550 nm.

Two methods have been proposed to reduce IC-XT without enlarging core pitch or reducing A_{eff}. One approach is to introduce a low-index layer, such as index trenches [15] or air holes [16], to surround each core. Air-holes have the largest index contrast and confine light more strongly than an index trench. However, it can be difficult during the drawing process to maintain their size. In addition, air-holes at a splice point can easily collapse, causing variation of the mode field diameter (MFD) and large splice loss. Index-trench technique is widely used in bending insensitive fibers to improve the bending-loss characteristics of a fiber. It can be fabricated by doping fluorine into the cladding. One issue with this structure is that the cutoff wavelength of the inner core lengthens rapidly if the core pitch becomes smaller than a certain threshold [15], because the confinement of the modes in the inner core is increased by the index trench of the surrounding cores. Fig. 2 shows the calculated LP_{21}-mode 22-m cutoff wavelength ($\lambda_{cc\text{-}21}$) of the center core of a two-LP-mode seven-core fiber as a function of core pitch [17]. The core parameters are shown in Fig. 3. A full vector finite element method was used for the calculation [18]. The $\lambda_{cc\text{-}21}$ increases rapidly when the core pitch is less than 45 μm. The core pitch of a trench assisted FM-MCF is thus also limited by the cutoff wavelength, not only by the IC-XT.

Another approach involves employing a heterogeneous core arrangement with cores of different relative effective index (n_{eff}). Fig. 4 illustrates the IC-XT behavior between the same propagation modes of a homogeneous MCF and a heterogeneous MCF as a function of the bending radius. The IC-XT of a homogeneous MCF changes proportionally as the bending radius increases. In the case of a heterogeneous MCF, the IC-XT changes radically at a threshold bending radius (R_{pk}) given by

$$R_{pk} = \frac{n_{eff}}{n_{eff}}\Lambda,$$

where n_{eff} is the effective index of a propagating mode in a core, Δn_{eff} is the difference of n_{eff} between cores, and Λ is the core pitch [13]. In the range of bending radius greater than R_{pk}, IC-XT is drastically reduced compared to a homogeneous MCF because the phases do not match. We can thus reduce the IC-XT of an MCF by setting R_{pk} below the effective bending radii in the cables. However, heterogeneous A_{eff} is not preferable because it leads to equalizing splice loss and optical signal-to-noise ratio (OSNR) over all cores, An SM-MCF with heterogeneous n_{eff} and homogeneous A_{eff} that has overcome these issues was reported [19].

Issue B is related to issue A. In the case of using an MCF in an actual transmission line, all cores are assumed to be excited equally and each core receives IC-XT from all neighboring cores. The aggregated IC-XT, IC-XT_{worst}, is calculated by

$$\text{IC-XT}_{worst} = \text{IC-XT} + 10 \cdot \log n,$$

where n is the number of neighboring cores surrounding each core. A small n is preferable to suppress IC-XT_{worst}. In order to both maximize the core count of an MCF and reduce n, various core layouts have been proposed for SM-MCFs, and some of these are also used for FM-MCFs. Fig. 5 summarizes the MCF core layouts presented to date: hexagonal close-packed structure (HCPS), one-ring structure (ORS) [20], dual-ring structure (DRS) [21], and square lattice structure (SLS) [22].

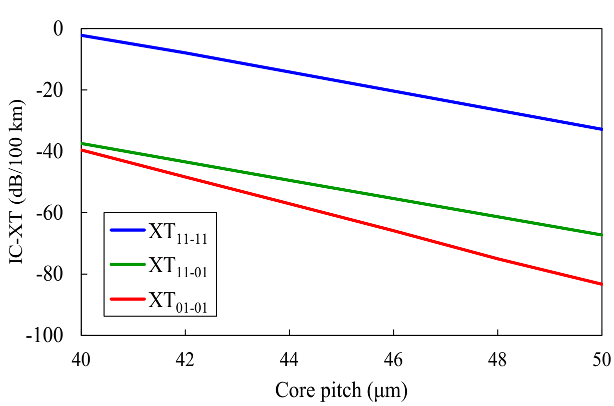

Fig. 1. Calculated IC-XT as a function of core pitch after 100 km propagation. Bending diameter is 210 mm, and wavelength is 1550 nm.

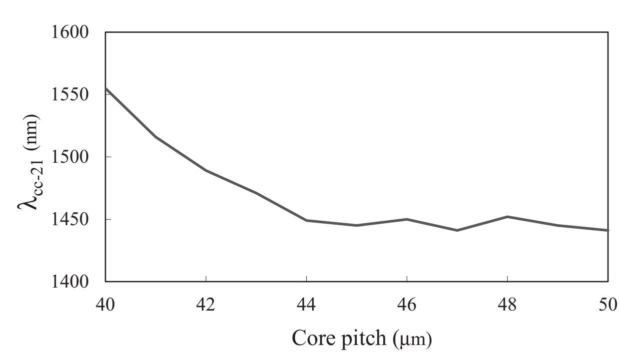

Fig. 2. Calculated 22-m LP_{21}-mode cutoff wavelength ($\lambda_{cc\text{-}21}$) of the center core of a two-LP-mode seven-core fiber as a function of core pitch.

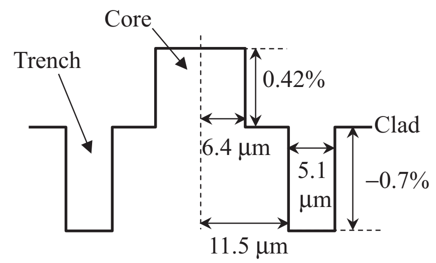

Fig. 3. Schematic of a core structure and core parameters used in the calculation of $\lambda_{cc\text{-}21}$.

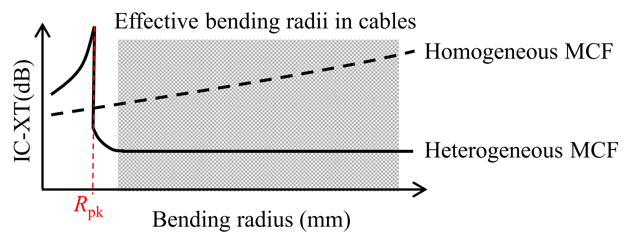

Fig. 4. Schematic of the dependence of bending diameter of IC-XT of a heterogeneous MCF and a homogeneous MCF.

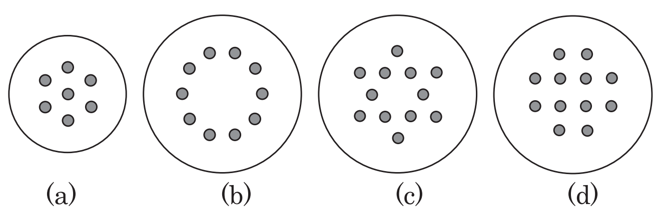

Fig. 5. Core layouts proposed previously: (a) HCPS (b) ORS (c) DRS (d) SLS.

Issues C and D originate from the few-mode core design. When degenerate modes, such as the LP_{11a} and LP_{11b}, are used as independent channels in an FMF, multi-input multi-output (MIMO) technology is typically used to separate the coupled degenerate modes at the output. The signal-recovery computation becomes more complex with increasing DMD. To reduce the signal-processing load for MIMO across wide range of wavelength, both low DMD magnitude and low DMD slope are desired. It is also important that there is a large difference in n_{eff} between different LP-modes in a core, as this serves to suppress IM-XT. There are two methods to reduce the DMD while maintaining small IM-XT. One is the optimization of refractive index profiles to minimize the DMD of a fiber. Fig. 6 summarizes index profiles presented in previous FMFs and FM-MCFs. The step-index profile results in a small IM-XT and large DMD [14]. In addition, the multi-step index profile (MSI) [23], graded-index (GI) profiles, and GI with an index trench can successfully suppress DMD [24,25]. The other approach is the DMD compensation line, which is a similar concept to a wavelength dispersion compensation line. Although a DMD compensation line requires positive and negative DMD FMFs, controlling DMD is realized by adjusting the length of each FMFs. Therefore, it has the benefit of being relatively insensitive to variations in the fabrication process.

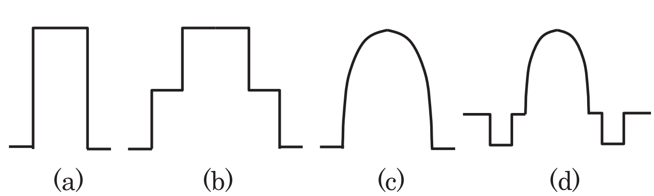

Fig. 6. Various core structures: (a) step-index (b) MSI (c) GI (d) GI with trench.

The combination of mode count and core count is decided by considering these issues. The core count is determined by the required IC-XT under the limitation of D_c. Controlling DMD of FMFs becomes more difficult as mode count increases, as the DMD of an FMF tends to be quite sensitive to structural fluctuations in the fabrication process. It is also reported that attenuation of an FMF increases as mode count increases [26]. FM-MCFs are required to have large SCC and to be designed with these issues being taken into account. Therefore, various types of FM-MCF are proposed.

3. Reported FM-MCFs

Table 1 summarizes the FM-MCFs reported to date. Relative core multiplicity factor (RCMF) [12] and relative spatial efficiency (RSE) [27] have been proposed to compare characteristics of FM-MCFs. The RCMF indicates how a large optical signal to noise ratio (OSNR) can be realized, which is given by the core multiplicity factor (CMF) of an MCF and that of a standard SMF. The CMF is the aggregate A_{eff} at 1550 nm of each mode in each core of an MCF as per the following equations,

$$RCMF = CMF_{MCF}/CMF_{SMF},$$

$$CMF_{MCF} = \frac{n\sum_{l}^{m} A_{eff-l}}{(\pi/4)D_c^2}$$

$$CMF_{SMF} = A_{eff-SMF}/D_{c-SMF} = 80/((\pi/4)125^2)$$

,where n is the core count, m is the mode count, and $A_{eff\text{-}l}$ is the A_{eff} of the l-th mode in each core. RSE indicates how many SCCs are realized in a limited D_c compared to an SMF, which is given by

$$RSE = \frac{m \times n}{D_c^2} \cdot 125^2.$$

The highest SCC of any reported SM-MCF to date is 32 [28]. In contrast, an SCC of over 100 was realized by using six-mode (LP_{01}, LP_{11a}, LP_{11b}, LP_{21a}, LP_{21b}, and LP_{02}) 19-core fibers [8–10]. However, the transmission distance of experiments using fibers with an SCC over 100 was limited to less than 10 km. In addition, the D_c of these fibers exceeded 300 μm. An RCMF of around 60 was achieved by a six-mode 19-core fiber with a D_c of less than 250 μm. A three-mode 12-core fiber realized DMD of less than 63 ps/km and an IC-XT_{worst} of −48.4 dB/500 km, which enabled a long distance QPSK transmission of 527 km [11].

4. Fiber design

For long-haul transmission using an FM-MCF, it is preferable to realize low DMD and low IC-XT. In order to realize these characteristics, we adopted a GI profile, heterogeneous core arrangement, and square lattice structure for the three-mode 12-core fiber.

4.1. Core design

It is desirable for the R_{pk} of IC-XT of a heterogeneous MCF to be small to suppress the deterioration of IC-XT in cables that have an effective radius of several hundred mm. A large Δn_{eff} is required to minimize R_{pk}. This large Δn_{eff} is realized by using a higher-n_{eff} core and a lower-n_{eff} core. Cores used in two-LP-mode MCFs must support both LP01- and LP11-mode transmissions over the C + L band. We used an effective two-LP-mode condition to realize these criteria, i.e., a cutoff wavelength of the LP21 mode of less than 1530 nm, and a bending loss of the LP11 mode of less than 0.5 dB/100 turns

Table 1
Various proposed FM-MCFs.

Refs.	Core count	Mode count	SCC	Core layout	Core profile	LP_{01}-A_{eff}* (μm^2)	IC-XT_{worst} (dB/100 km)	D_c (μm)	RCMF	RSE	DMD*	Fiber length (km)
[29]	4	3	12	SLS	Step	112.7	−39*	176	11.5	6.1	3000	3.7
[30]	14	1 or 3	18	HCPS	–	–	–	–	–	–	–	1
[31]	6	3	18	HCPS	GI + Trench	64	–	125	24.7	18	520	10
[32]	7	3	21	HCPS	Step + Trench	183	−25*	243	18.1	5.9	–	1.0
[33][34]	7	3	21	HCPS	Step + Air-holes	113	−12*	192	16.8	8.9	4600	1
[17]	7	3	21	HCPS	Step + Trench	110	−40*	195	16.6	8.6	2729	2.0
[35][36]	12	3	36	SLS	MSI + Trench	96	−59*	230	16.8	10.7	530	40.4
[11]	12	3	36	SLS	GI + Trench	110	−55*	230	16.5	10.6	63	52.7
[37]	19	3	57	HCPS	Step + Trench	218	−7*	440	15.8	4.6	–	0.12
[38]	12	6	72	SLS	GI + Trench	87	−27**	227	22	21.8	430	4.2
[8][39]	36	3	108	HCPS	Step + Trench	76	−5*	306	21.6	18.0	7400	5.5
[9][40][41]	19	6	114	HCPS	GI + Trench	64.3	−80*	318	30.1	17.6	950	9.76
[10]	19	6	114	HCPS	GI + Trench	80.1	−30.8**	246	60.3	29.4	330	8.85

* Measured at 1550 nm.
** Measured at 1565 nm.

at a wavelength of 1625 nm and a bending radius of 30 mm. Too high n_{eff} causes increasing cutoff wavelength of the LP21 mode and too low an n_{eff} causes deterioration of the bending loss of the LP11 mode under the equal trench width condition. Using only two types of core is essential to maximize Δn_{eff} under the limitations of the effective two mode conditions. Fig. 7 shows a schematic of a GI profile with an index-trench. The n_{eff} and A_{eff} of a core are determined by Δ and r_1, respectively. The DMD magnitude and slope are mainly affected by α and r_2. The two core profiles, which were used to realize a heterogeneous core arrangement by the minimum core types, were optimized in terms of DMD, DMD slope, and n_{eff}. Fig. 8 shows the structural core-parameter dependence of the DMD, n_{eff}, and A_{eff} at 1550 nm when W/r_1 is 0.7 and W/r_1 is 0.2. Here, we define DMD as positive when the transmission speed of the LP01 mode is faster than that of the LP11 mode. White lines, black lines, black dotted lines, and black dash lines show the effective two-LP-mode conditions, LP_{01}-A_{eff}, n_{eff}, and DMD of zero, respectively. We can choose two cores (Core 1 and Core 2) which satisfy the effective two-LP-mode condition and homogeneous A_{eff} of 110 μm^2. This large Aeff is helpful for suppressing non-linearity. The core parameters used in the following calculations are summarized in Table 2. Fig. 9 shows the calculated DMD as a function of wavelength. It is confirmed that these cores can achieve a DMD of less than |100| ps/km over the range of the C + L band.

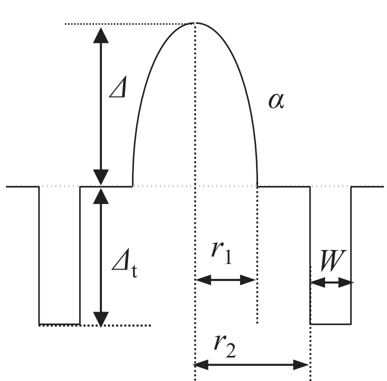

Fig. 7. Schematic of a GI profile with index-trench.

4.2. Core pitch optimization

The IC-XT of a MCF over the range of R_{pk} is dominated by correlation length as

$$\text{IC-XT} = \frac{2\kappa^2}{d\Delta\beta^2}L,$$

where κ is the coupling coefficient, β is the difference of the propagation constant of the two cores, L is the fiber length, and d is the correlation length [13]. We used a value of d of 50 mm. Fig. 10 shows the calculated IC-XT after 500-km propagation as a function of Λ at 1565 nm and at a bending diameter of 500 mm. Λ of larger than 43 μm realizes IC-XT of less than −40 dB/500 km. Fig. 11 shows calculated bending radius dependence of $XT_{11\text{-}11}$ when Λ is 43 μm. An R_{pk} of less than 100 mm is achieved owing to the large Δn_{eff}, enabling the fiber to be used with a variety of cable types without crosstalk degradation [42].

4.3. Cladding thickness

Cladding thickness (T_c) is defined as the shortest distance from the center of the outmost core to the coating. Values of T_c that are too small cause excess losses owing to the leakage of the light into the coating. This phenomenon occurs in the LP_{11} mode rather than in the LP_{01} mode because the LP_{11} mode has far larger A_{eff} than the LP_{01} mode. Fig. 12 shows calculated LP_{11}-bending losses as a function of T_c at 1550, 1565, and 1625 nm. A bending loss of less than 0.001 dB/km at 1565 nm is required to avoid performance deterioration of the outermost cores. T_c of larger than 42.2 μm enable the suppression of the bending loss of both Core 1 and Core 2 to less than 0.001 dB/km. This large T_c is also helpful to sustain a low microbending loss.

4.4. Core layout

In the case of HCPS and DRS, three types of cores are required to allow the alternate arrangement of cores as shown in Fig. 13 (a) and (b). On the other hand, the ORS and SLS enable a heterogeneous arrangement with only two core types (Fig. 13(c) and (d), respectively). For an ORS, the relation for maximum containable core count (C), core pitch (Λ), D_c, and cladding thickness (T_c) is defined as

$$D_c = \frac{\Lambda}{\sin\frac{\pi}{C}} + 2 \times T_c,$$

Please cite this article in press as: Y. Sasaki et al., Few-mode multicore fibers for long-haul transmission line, Opt. Fiber Technol. (2016), http://dx.doi.org/10.1016/j.yofte.2016.09.017

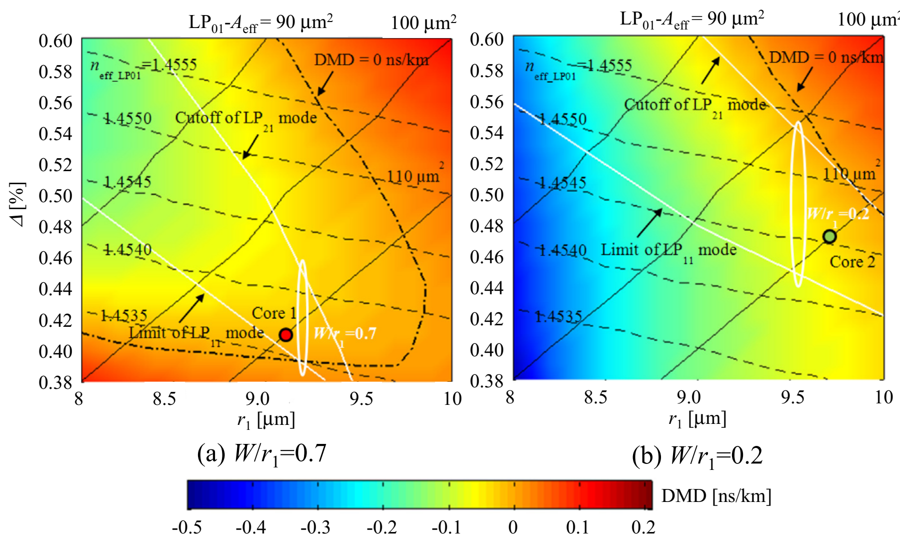

Fig. 8. Structural core parameter dependence of DMD, n_{eff}, and LP_{01}-A_{eff} when W/r_1 is 0.7 and W/r_1 is 0.2. White lines, black lines, and black dotted lines, and a black dashed line indicate effective two-LP-mode conditions, LP_{01}-A_{eff}, n_{eff} and DMD of zero, respectively.

Table 2
Optimized core parameters.

	Unit	Core 1	Core 2
r_1	µm	9.78	9.22
Δ	%	0.473	0.420
Δ_t	%	−0.70	−0.70
r_2/r_1	–	1.3	1.3
W/r_1	–	0.2	0.7
α	–	2.2	2.2
LP_{01}-A_{eff}*	µm^2	110.1	110.2
LP_{11}-A_{eff}*	µm^2	146.9	146.4

* Calculated value.

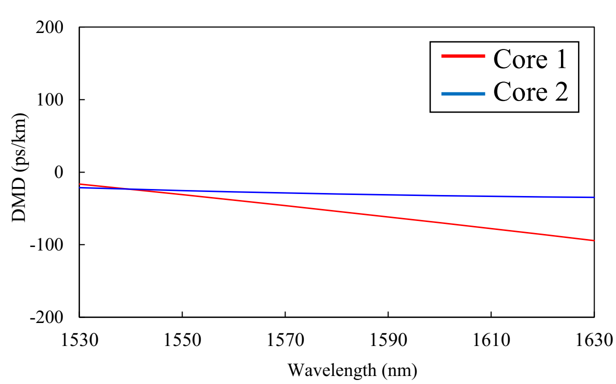

Fig. 9. Calculated wavelength dependence of DMD of Core 1 and Core 2.

For an SLS, the optimum core arrangement for minimizing D_c depends on the core count. The relations between C, Λ, D_c, and T_c in an SLS are:

$$D_c = \begin{cases} \sqrt{2} \times \Lambda + 2 \times T_c (C = 4) \\ \sqrt{5} \times \Lambda + 2 \times T_c (C = 5–6) \\ 2\sqrt{2} \times \Lambda + 2 \times T_c (C = 7–9) \\ \sqrt{10} \times \Lambda + 2 \times T_c (C = 10–12) \\ 3\sqrt{2} \times \Lambda + 2 \times T_c (C = 13–16) \end{cases}$$

Fig. 14 shows the relationship of D_c and C in the ORS and SLS. Λ and T_c are chosen to be 43.0 µm and 42.2 µm, respectively. By using the SLS, a core count of 12 is realizable in a D_c of 250 µm. Although a fiber with D_c of 250 µm is larger than a normal SMF with D_c of

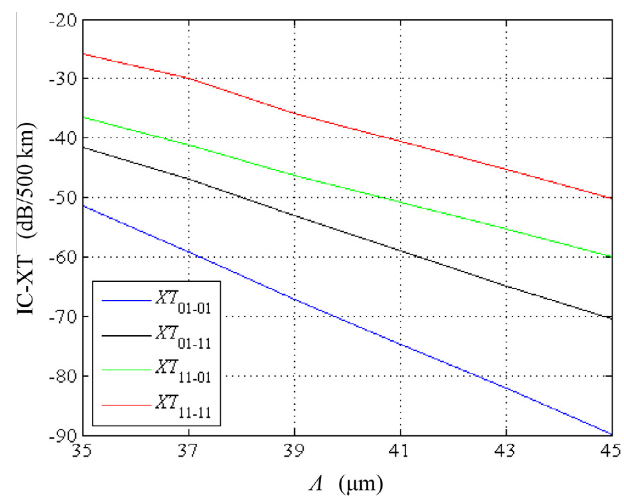

Fig. 10. Calculated IC-XT ($XT_{11\text{-}11}$, $XT_{01\text{-}11}$, $XT_{11\text{-}01}$, $XT_{01\text{-}01}$) as function of core pitch (Λ). Bending diameter is 500 mm and wavelength is 1565 nm.

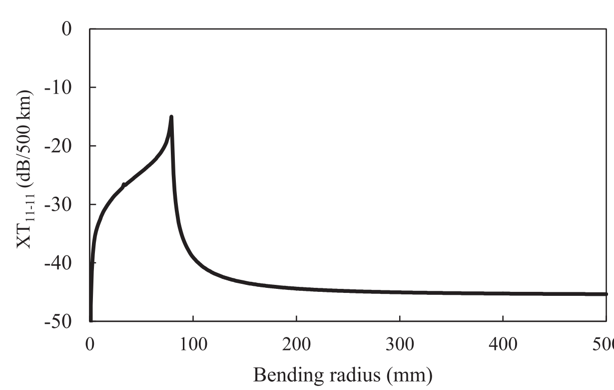

Fig. 11. Calculated bending radius dependence of $XT_{11\text{-}11}$. R_{pk} of less than 100 mm is realized.

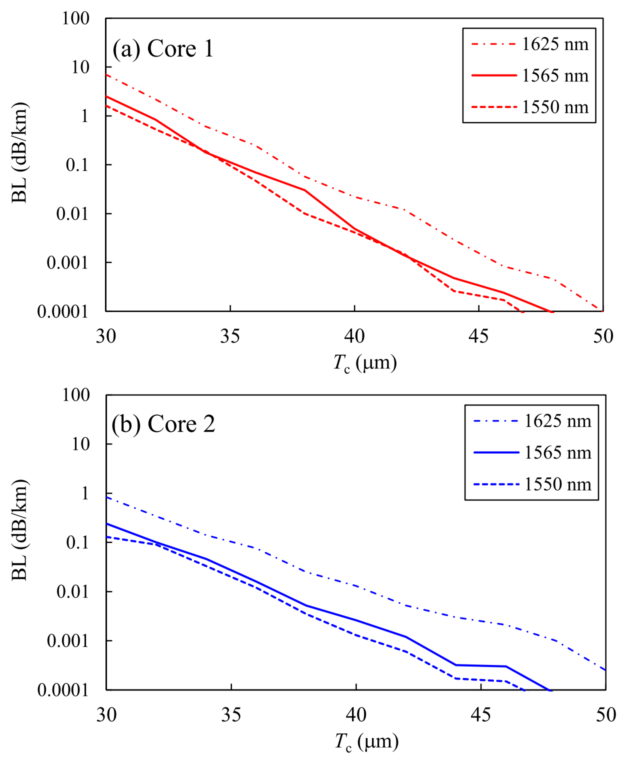

Fig. 12. Calculated bending loss of Core 1 and Core 2 as a function of cladding thickness.

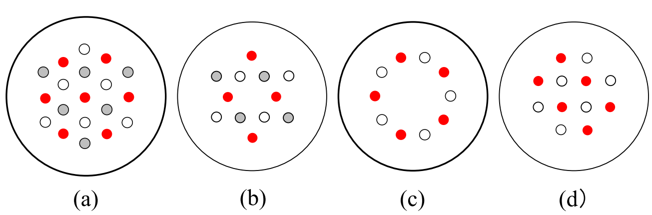

Fig. 13. Heterogeneous core arrangement with minimal core types in various core layouts: (a) HCPS. (b) DRS. (c) ORS. (d) SLS.

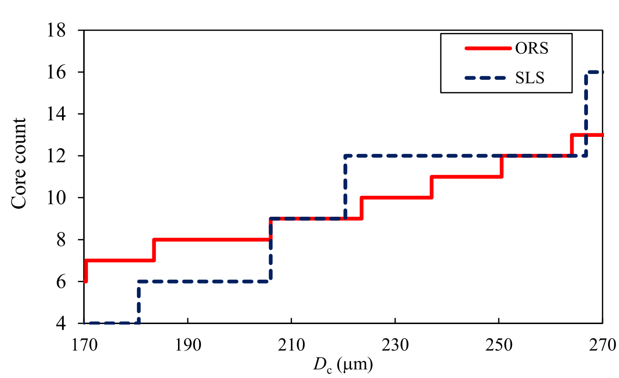

Fig. 14. Relationship of D_c and maximum containable core count in ORS and SLS. Λ and T_c are assumed to be 43 μm and 42.2 μm, respectively.

125 μm, a fiber with D_c of 250 μm can be used in a telecommunication network by using a proof level of more than 1% [2,10]. When using the SLS for a trench assisted MCF, the $\lambda_{cc\text{-}21}$ of the inner cores should be noted because they are surrounded by a maximum of seven cores. Fig. 15 shows the calculated $\lambda_{cc\text{-}21}$ of the inner cores. By setting Λ larger than 43 μm, lengthening of the $\lambda_{cc\text{-}21}$ is

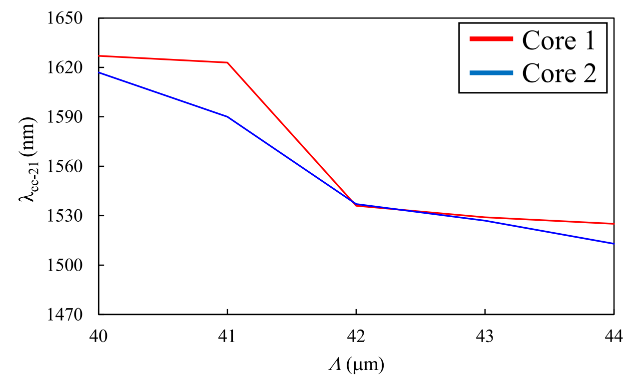

Fig. 15. Calculated $\lambda_{cc\text{-}21}$ of Core 1 and Core 2 in the inner layer as a function of core pitch.

avoidable even if we use the SLS. The optimized fiber parameters are summarized in Table 3.

5. Fiber fabrication

There are two main methods to fabricate MCFs, namely the drill tool method and the stack and draw method as shown in Fig. 16. The stack and draw method is suitable for fabricating large size preforms and low loss fibers [43]. We fabricated a 52.7-km three-mode 12-core fiber based on the fiber design using the stack and draw method. Fig. 17(a) shows a cross-section of the fabricated fiber. Fig. 17(b) illustrates the core number assignment. High n_{eff} cores with thin trench-width are marked blue and have odd number designations, and low n_{eff} cores with thick trench width are marked white and have even numbers. Table 4 summarizes the measured dimensions. The averaged Λ was almost identical to the designed value, and the T_c and coating diameter were 47 μm and 340.8 μm, respectively. Table 5 summarizes the optical characteristics of each core. Measured $\lambda_{cc\text{-}21}$s were less than 1530 nm for all cores.

Fig. 18 shows the setup for DMD measurement by the impulse response method. The excitation ratio of the LP_{01} and LP_{11} modes was controlled by adjusting the offset position of the SMF against each core of the fabricated fiber. Fig. 19 presents the wavelength dependence of DMD for all the cores. The symbols indicate measured DMD values. The lines indicate approximate linear fits from the measured values. The DMD values were estimated to be less than |63| ps/km over the C band for all cores, owing to the optimum GI profile. We then measured IC-XTs between adjacent cores of the 52.7-km fabricated fiber. Fig. 20 shows the setup for measuring the IC-XT values. The spool diameter of the fiber was 310 mm. A mode multiplexer (mode MUX) can convert the LP_{01} mode to a higher order mode such as the LP_{11} mode. The output port from a mode MUX that was connected to a tunable light source was spliced to a core of the fabricated fiber to excite both the LP_{11a} and LP_{11b} modes. The output powers from cores on another end face were measured with a two-LP-mode single-core fiber (TM-SCF). The TM-SCF had the same profile as the fabricated MCF (GI with trench) to measure the low IC-XT values [44]. The measured

Table 3
Optimized fiber parameters (μm).

Item	Λ	T_c	D_c
Value	43.0	42.2	220.4

Please cite this article in press as: Y. Sasaki et al., Few-mode multicore fibers for long-haul transmission line, Opt. Fiber Technol. (2016), http://dx.doi.org/10.1016/j.yofte.2016.09.017

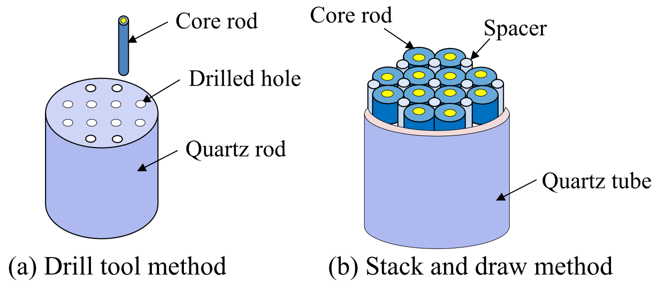

Fig. 16. Fabrication methods of MCFs.

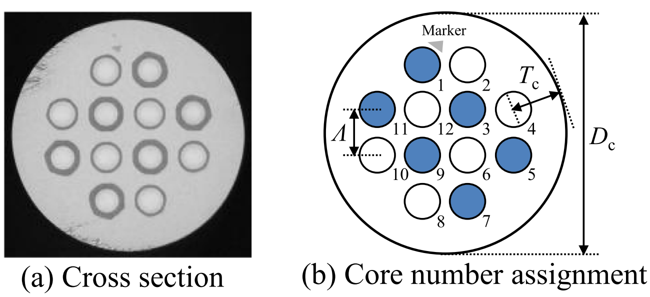

Fig. 17. Cross-section and core number assignment of the fabricated fiber. Blue-marked cores are high n_{eff} cores and white-marked cores are low n_{eff} cores. (For interpretation of the references to colour in this figure legend, the reader is referred to the web version of this article.)

Table 4
Measured dimensions of the fabricated fiber (μm).

	Ave.	Max.	Min.
D_c	229.8	230.4	229.0
Λ	43.0	43.4	42.8

values of IC-XT ware less than −60 dB/span in the C + L band. Fig. 21 shows the estimated IC-XT_{worst} after 500 km propagation

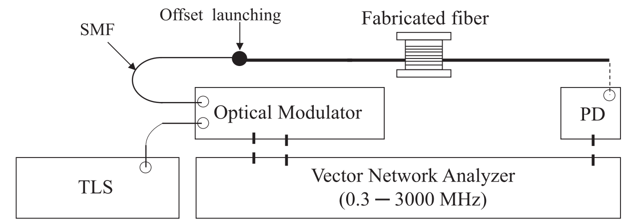

Fig. 18. Setup for the measurement of impulse responses. (TLS: tunable light source, PD: photo detector).

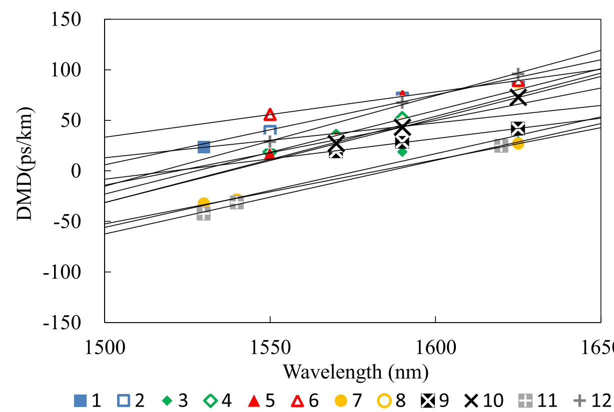

Fig. 19. Measured wavelength dependence of DMD of each core. Symbols are measured values, and lines are linear approximations.

at 1550 nm and 1608 nm. The IC-XT might be smaller than the measurement limits of our system because there was no IC-XT dependency on wavelength. However, it was confirmed that the largest IC-XT_{worst} was −48.4 dB/500 km at 1550 nm. This value was much smaller than the calculated value. IC-XT over R_{pk} of a heterogeneous MCF is dominated by the correlation length [13]. There is a possibility that the correlation length of the fabricated fiber was different from the assumed value of 50 mm.

Table 5
Measured optical characteristics of the fabricated fiber.

	Unit	Mode	Core	Wavelength	Ave.	Max.	Min.
Attenuation	dB/km	LP_{01}	1	1550 nm	0.219	0.220	0.218
				1625 nm	0.220	0.221	0.220
			2	1550 nm	0.217	0.221	0.216
				1625 nm	0.223	0.224	0.222
A_{eff}	μm^2	LP_{01}	1	1550 nm	109.9	111.4	108.2
				1625 nm	116.1	118.0	113.4
			2	1550 nm	109.3	111.0	108.2
				1625 nm	115.3	117.3	114.5
		LP_{11}***	1	1550 nm	155.2	155.8	154.7
			2		152.4	152.9	151.9
MFD	μm	LP_{01}	1	1550 nm	11.8	11.9	11.7
				1625 nm	12.2	12.2	12.0
			2	1550 nm	11.7	11.9	11.4
				1625 nm	12.1	12.2	12.1
22-m cutoff wavelength	nm	LP_{21}	1	–	1504	1522	1492
			2		1392	1414	1376
PMD* on the spool	ps/$\sqrt{}$km	LP_{01}	1	C + L band	0.43	0.91	0.12
			2		0.55	1.36	0.16
PDL** on the spool	dB	LP_{01}	1	C + L band	0.94	1.39	0.59
			2		1.10	1.65	0.27
Chromatic dispersion	ps/nm/km	LP_{01}	1	1550 nm	19.49	19.52	19.47
			2		20.04	20.06	20.02

* Polarization mode dispersion.
** Polarization dependent loss.
*** Calculated value.

Please cite this article in press as: Y. Sasaki et al., Few-mode multicore fibers for long-haul transmission line, Opt. Fiber Technol. (2016), http://dx.doi.org/10.1016/j.yofte.2016.09.017

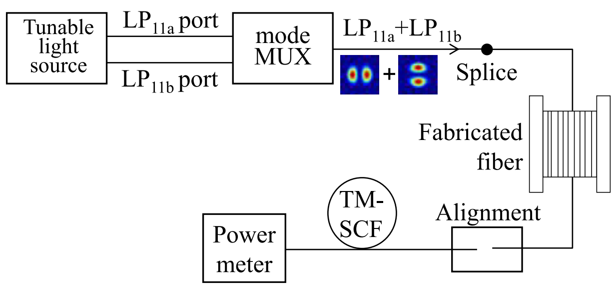

Fig. 20. A setup for measuring IC-XT of the fabricated fiber. Both LP_{11a} and LP_{11b} modes were excited by a mode MUX.

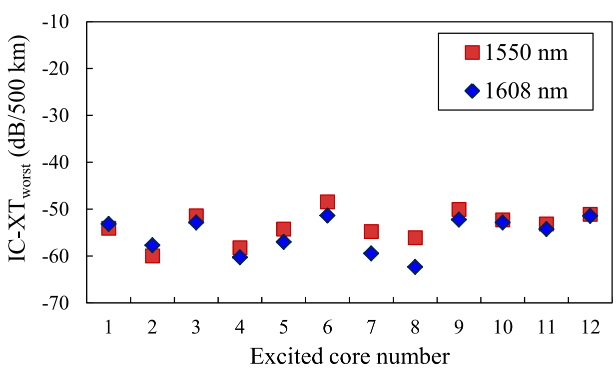

Fig. 21. Estimated IC-XT_{worst} after 500-km propagation using measured IC-XT of one-span fiber at 1550 nm and 1608 nm.

6. Conclusion

Issues required for designing FM-MCFs were discussed. Furthermore, reported FM-MCFs were reviewed. A lot of FM-MCFs including SCC of over 100 have been proposed.

The fiber design and characteristics of the fabricated three-mode 12-core fiber used in a long-haul transmission experiment were described. Low DMD of |63| ps/km in C-band was achieved by optimization of GI core profile. The IC-XT_{worst} of −48.4 dB after 500-km propagation was realized by a heterogeneous core arrangement. A square lattice structure enabled the coexistence of this low IC-XT and an SCC of 36 within a D_c of 230 µm. Further research will enable the enhancement of SCC in FM-MCFs while retaining characteristics such as low IC-XT, low DMD, and small D_c, which are required for long-haul DSDM transmission.

Acknowledgement

This work was partially supported by National Institute of Information and Communications Technology (NICT), Japan.

References

[1] E.B. Desurvire, Capacity demand and technology challenges for lightwave systems in the next two decades, J. Lightwave Technol. 24 (2006) 4697–4710.
[2] S. Matsuo, K. Takenaga, Y. Sasaki, Y. Amma, S. Saito, K. Saitoh, T. Matsui, K. Nakajima, T. Mizuno, H. Takara, Y. Miyamoto, T. Morioka, High-spatial-multiplicity multicore fibers for future dense space-division-multiplexing systems, J. Lightwave Technol. 34 (2016) 1464–1475.
[3] H. Takara, A. Sano, T. Kobayashi, H. Kubota, H. Kawakami, A. Matsuura, Y. Miyamoto, Y. Abe, H. Ono, K. Shikama, Y. Goto, K. Tsujikawa, Y. Sasaki, I. Ishida, K. Takenaga, S. Matsuo, K. Saitoh, M. Koshiba, T. Morioka, 1.01-Pb/s (12 SDM/222 WDM/456 Gb/s) crosstalk-managed transmission with 91.4-b/s/Hz aggregate spectral efficiency, in: Proc. of Eur. Conf. Exhib. Opt. Commun., Amsterdam, Netherlands, 2012, Paper Th.3.C.1.
[4] T. Kobayashi, H. Takara, A. Sano, T. Mizuno, H. Kawakami, Y. Miyamoto, K. Hiraga, Y. Abe, H. Ono, M. Wada, Y. Sasaki, I. Ishida, K. Takenaga, S. Matsuo, K. Saitoh, M. Yamada, H. Masuda, T. Morioka, 2 × 344 Tb/s propagation-direction interleaved transmission over 1500-km MCF enhanced by multicarrier full electric-field digital back-propagation, in: Proc. of Eur. Conf. Exhib. Opt. Commun., London, U.K., Sept. 2013, Paper PD3.E.4.
[5] K. Igarashi, T. Tsuritani, I. Morita, Y. Tsuchida, K. Maeda, M. Tadakuma, T. Saito, K. Watanabe, K. Imamura, R. Sugizaki, M. Suzuki, 1.03-Exabit/s·km super-nyquist-WDM transmission over 7326-km seven-core fiber, in: Proc. of Eur. Conf. Exhib. Opt. Commun., London, U.K., Sept. 2013, Paper PD3.E.3.
[6] B.J. Puttnam, R.S. Luis, W. Klaus, J. Sakaguchi, J.-M. Deigado Mendinueta, Y. Awaji, N. Wada, Y. Tamura, T. Hayashi, M. Hirano, J. Marciante., 2.15 Pb/s transmission using a 22 core homogeneous single-mode multi-core fiber and wideband optical comb, in: Proc. of Eur. Conf. Exhib. Opt. Commun., Valencia, Spain, Sept. 2015, Paper PDP3.1.
[7] R. Ryf, H. Chen, N.K. Fontsine, A.M. Velazquez-Benitez, Jose Antonio-López, C. Jin, B. Huang, M. Bigot-Astruc, D. Moiln, F. Achten, P. Sillard, R. Amezcua-Correa, 10-mode mode-multiplexed transmission over 125-km single-span multimode fiber, in: Proc. of Eur. Conf. Exhib. Opt. Commun., Valencia, Spain, Sept. 2015, Paper PDP3.3.
[8] J. Sakaguchi, W. Klaus, J.-M.D. Mendinueta, B.J. Puttnam1, R.S. Luis, Y. Awaji1, N. Wada, T. Hayashi, T. Nakanishi, T. Watanabe, Y. Kokubun, T. Takahata, T. Kobayashi, Realizing a 36-core, 3-mode fiber with 108 spatial channels, in: Proc. of Opt. Fiber Commun. Conf., Los Angeles, CA, USA, 2015, Paper Th5C.2.
[9] K. Igarashi, D. Souma, Y. Wakayama, K. Takeshima, Y. Kawaguchi, T. Tsuritani, I. Morita, M. Suzuki, 114 space-division-multiplexed transmission over 9.8-km weakly-coupled-6-mode uncoupled-19-core fibers, in: Proc. of the Opt. Fiber Commun. Conf., Los Angeles, CA, USA, 2015, Paper Th5C.4.
[10] T. Sakamoto, T. Matsui, K. Saitoh, S. Saitoh, K. Takenaga, T. Mizuno, Y. Abe, K. Shibahara, Y. Tobita, S. Matsuo, K. Aikawa, S. Aozasa, K. Nakajima, Y. Miyamoto, Low-loss and low-DMD few-mode multi-core fiber with highest core multiplicity factor, in: Proc. of Opt. Fiber Commun. Conf., Anaheim, CA, USA, 2016, Paper Th5A.2.
[11] K. Shibahara, T. Mizuno, H. Takara, A. Sano, H. Kawakami, D. Lee, Y. Miyamoto, H. Ono, M. Oguma, Y. Abe, T. Kobayashi, T. Matsui, R. Fukumoto, Y. Amma, T. Hosokawa, S. Matsuo, K. Saito, H. Nasu, T. Morioka, Dense SDM (12-core × 3-mode) transmission over 527 km with 33.2-ns mode-dispersion employing low-complexity parallel MIMO frequency-domain equalization, in: Proc. of at the Opt. Fiber Commun. Conf., Los Angeles, CA, USA, 2015, Paper Th5C.3.
[12] K. Takenaga, Y. Sasaki, N. Guan, S. Matsuo, M. Kasahara, K. Saitoh, M. Koshiba, A large-effective-area few-mode multi-core fiber, IEEE Photon. Technol. Lett. 24 (2012) 1941–1944.
[13] M. Koshiba, K. Saitoh, K. Takenaga, S. Matsuo, Multi-core fiber design and analysis: coupled-mode theory and coupled-power theory, Opt. Express 19 (2011) B102–B111.
[14] P. Sillard, M. Bigot-Astruc, D. Boivin, H. Maerten, L. Provost, Few-mode fiber for uncoupled mode-division multiplexing transmissions, in: Proc. of the Eur. Conf. Exhib. Opt. Commun., Torino, Italy, Sept. 2011, Paper Tu.5.LeCervin.7.
[15] K. Takenaga, Y. Arakawa, S. Tanigawa, N. Guan, S. Matsuo, K. Saitoh, M. Koshiba, Reduction of crosstalk by trench-assisted multi-core fiber, in: Proc. of the Opt. Fiber Commun. Conf./Nat. Fiber Opt. Eng. Conf., Los Angeles, CA, USA, Mar. 2011, Paper OWJ4.
[16] T. Sakamoto, K. Saitoh, N. Hanzawa, K. Tsujikawa, L. Ma, M. Koshiba, F. Yamamoto, Crosstalk suppressed hole-assisted 6-core fiber with cladding diameter of 125 µm, in: Proc. of Eur. Conf. Exhib. Opt. Commun., London, Sept. 2013, Paper Mo.3.A.3.
[17] Y. Sasaki, Y. Amma, K. Takenaga, S. Matsuo, K. Saitoh, M. Koshiba, Trench-assisted low-crosstalk few-mode multicore fiber, in: Proc. of Eur. Conf. Exhib. Opt. Commun., London, Sept. 2013, Paper Mo.3.A.5.
[18] K. Saitoh, M. Koshiba, Full-vectorial imaginary-distance beam propagation method based on a finite element scheme: Application to photonic crystal fibers, IEEE J. Quantum Elect. 38 (2002) 927–933.
[19] K. Saitoh, M. Koshiba, K. Takenaga, S. Matsuo, Low-crosstalk multi-core fibers for long-haul transmission, SPIE 8284 (2012) 8240I.
[20] S. Matsuo, Y. Sasaki, T. Akamatsu, I. Ishida, K. Takenaga, K. Okuyama, K. Saitoh, M. Koshiba, 12-core fiber with one ring structure for extremely large capacity transmission, Opt. Express 20 (2012) 28398–28408.
[21] K. Takenaga, Multicore fiber with dual-ring structure, in: Proc. of OptoElectronics and Communication Conf./Australian Conf. on Optical Fibre Technol., Melbourne, July 2014, Paper MO1E-5.
[22] F. Ye, K. Saitoh, H. Takara, R. Asif, T. Morioka, High-count multi-core fibers for space-division multiplexing with propagation-direction interleaving, in: Proc. of Opt. Fiber Commun. Conf., Los Angeles, CA, USA, 2015, Paper Th4C.3.
[23] T. Sakamoto, T. Mori, T. Yamamoto, S. Tomita, Differential mode delay managed transmission line for WDM-MIMO system using multi-step index fiber, J. Lightwave Technol. 30 (2012) 2783–2787.
[24] P. Sillard, D. Molin, M. Bigot-Astruc, H. Maerten, D. Van Ras, F. Achten, Low-DMGD 6-LP-Mode Fiber, in: Proc. of Opt. Fiber Commun. Conf./Nat. Fiber Opt. Eng. Conf., San Francisco, CA, USA, Mar. 2014, Paper M3F.2.
[25] T. Mori, T. Sakamoto, M. Wada, T. Yamamoto, F. Yamamoto, Six-LP-mode transmission fiber with DMD of less than 70 ps/km over C + L band, in: Proc. of Opt. Fiber Commun. Conf./Nat. Fiber Opt. Eng. Conf., San Francisco, CA, Mar. 2014, Paper M3F.3.
[26] P. Sillard, D. Molin, M. Bigot-Astruc, A. Amezcua-Correa, K. de Jongh, F. Achten, 50 µm multimode fibers for mode division multiplexing, in: Proc. of Eur. Conf. Exhib. Opt. Commun., Valencia, Spain, Sept. 2015, Paper Mo.4.1.2.
[27] K. Saitoh, S. Matsuo, Multicore fiber technology, J. Lightwave Technol. 34 (2016) 55–66.

Please cite this article in press as: Y. Sasaki et al., Few-mode multicore fibers for long-haul transmission line, Opt. Fiber Technol. (2016), http://dx.doi.org/10.1016/j.yofte.2016.09.017

[28] T. Mizuno, K. Shibahara, H. Ono, Y. Abe, Y. Miyamoto, F. Ye, T. Morioka, Y. Sasaki, Y. Amma, K. Takenaga, S. Matsuo, K. Aikawa, K. Saitoh, Y. Jung, D.J. Richardson, K. Pulverer, M. Bohn, M. Yamada, 32-core dense SDM unidirectional transmission of PDM-16QAM signals over 1600 km using crosstalk-managed single-mode heterogeneous multicore transmission line, in: Proc. of Opt. Fiber Commun. Conf., Los Angeles, CA, USA, 2016, Paper Th5C.3.

[29] Y. Sasaki, K. Takenaga, N. Guan, S. Matsuo, K. Saitoh, M. Koshiba, Large-effective-area uncoupled few-mode multi-core fiber, Opt. Express 20 (2012) B77–B84.

[30] D. Qian, E. Ip, M.F. Huang, M.J. Li, A. Dogariu, S. Zhang, Y. Shao, Y.K. Huang, Y. Zhang, X. Cheng, Y. Tian, P. Ji, A. Collier, Y. Geng, J. Linares, C. Montero, V. Moreno, X. Prieto, T. Wang, 1.05 Pb/s transmission with 109b/s/Hz spectral efficiency using hybrid single- and few-mode cores, in: Proc. of Frontiers Opt., Rochester, NY, USA, 2012, Paper FW6C.

[31] T. Sakamoto, T. Mori, T. Yamamoto, M. Wada, F. Yamamoto, Moderately coupled 125-μm cladding 2 LP-mode 6-core fiber for realizing low MIMO-DSP and high spatial density, in: Proc. of the Eur. Conf. Opt. Commun., Canne, France, 2014, Paper Tu.4.1.3.

[32] K. Mukasa, K. Imamura, R. Sugizaki, 7-core 2-mode fibers with large Aeff to simultaneously realize "3M", in: Proc. of OptoElectron. Commun. Conf., Busan, Korea, 2012, Paper 5C1-1.

[33] C. Xia, R. Amezcua-Correa, N. Bai, E. Antonio-Lopez, D.M. Arrioja, A. Schulzgen, M. Richardson, J. Linares, C. Montero, E. Mateo, X. Zhou, G. Li, Hole-assisted few-mode multicore fiber for high-density space-division multiplexing, IEEE Photon. Technol. Lett. 24 (2012) 1914–1917.

[34] R.G.H. van Uden, R. Amezcua Correa, E. Antonio-Lopez, F.M. Huijskens, G. Li, A. Schülzgen, H. de Waardt, A.M.J. Koonen, C.M. Okonkwo, 16QAM SDM-WDM transmission over a novel hole-assisted few-mode multi-core fiber, in: Proc. of IEEE Photonics Society Summer Topical Meeting Ser., Montreal, QC, Canada, Jul. 2014, Paper ME3.2.

[35] T. Mizuno, T. Kobayashi, H. Takara, A. Sano, H. Kawakami, T. Nakagawa, Y. Miyamoto, Y. Abe, T. Goh, M. Oguma, T. Sakamoto, Y. Sasaki, I. Ishida, K. Takenaga, S. Matsuo, K. Saitoh, T. Morioka, 12-core $\times$ 3-mode dense space division multiplexed transmission over 40 km employing multi-carrier signals with parallel MIMO equalization, in: Proc. of Opt. Fiber Commun. Conf., San Francisco, CA, USA, 2014, Paper Th5B.2.

[36] Y. Sasaki, Y. Amma, K. Takenaga, S. Matsuo, K. Saitoh, M. Koshiba, Few-mode multicore fiber with 36 spatial modes (three modes (LP_{01}, LP_{11a}, LP_{11b}) $\times$ 12 Cores), J. Lightwave Technol. 33 (2015) 964–970.

[37] K. Mukasa, K Imamura, R. Sugizaki, Multi-core few-mode optical fibers with large Aeff, in: Proc. of Eur. Conf. Opt. Commun., Amsterdam, Netherlands, 2012, Paper P1.08.

[38] T. Sakamoto, T. Matsui, K. Saitoh, S. Saitoh, K. Takenaga, S. Matsuo, Y. Tobita, N. Hanzawa, K. Nakajima, F. Yamamoto, Few-mode multi-core fibre with highest core multiplicity factor, in: Proc. of Eur. Conf. Exhib. Opt. Commun., Valencia, Spain, Sept. 2015, Paper We.1.4.3.

[39] J. Sakaguchi, W. Klaus, J.-M.D. Mendinueta, B.J. Puttnam, R.S. Luis, Y. Awaji, N. Wada, T. Hayashi, T. Nakanishi, T. Watanabe, Y. Kokubun, T. Takahata, T. Kobayashi, Large spatial channel (36-core $\times$ 3-mode) heterogeneous few-mode multicore fiber, J. Lightwave Technol. 34 (2016) 93–102.

[40] D. Soma, K. Igarashi, Y. Wakayama, K. Takeshima, Y. Kawaguchi, N. Yoshikane, T. Tsuritani, I. Morita, M. Suzuki, 2.05 Peta-bit/s super-nyquist WDM-SDM transmission using 9.8-kim 6-mode, 9-core fiber in full C band, in: Proc. of Eur. Conf. Exhib. Opt. Commun., Valencia, Spain, Sept. 2015, Paper PDP.3.2.

[41] T. Hayashi, T. Nagashima, K. Yonezawa, Y. Wakayama, D. Soma, K. Igarashi, T. Tsuritani, T. Sasaki, 6-mode 19-core fiber for weakly-coupled mode-multiplexed transmission over uncoupled cores, in: Proc. of Eur. Conf. Exhib. Opt. Commun., Valencia, Spain, Sept. 2015, Paper PDP3.2.

[42] N. Okada, M. Yamanaka, Y. Sato, H. Watanabe, O. Koyasu, M. Miyamoto, Study of the SZ-slotted rod type optical cable with the 4-fiber ribbons for aerial applications, in: Proc. of International Wire & Cable Symposium, Philadelphia, PA, Nov. 1997, pp. 785–792.

[43] I. Ishida, T. Akamatsu, Z. Wang, Y. Sasaki, K. Takenaga, S. Matsuo, Possibility of stack and draw process as fabrication technology for multi-core fiber, in: Proc. of Opt. Fiber Commun. Conf./Nat. Fiber Opt. Eng. Conf., Anaheim, CA, USA, Mar. 2013, Paper OTu2G.1.

[44] T. Hayashi, T. Taru, O. Shimakawa, T. Sasaki, E. Sasaoka, Characterization of crosstalk in ultra-low-crosstalk multi-core fiber, J. Lightwave Technol. 30 (2012) 583–589.

Please cite this article in press as: Y. Sasaki et al., Few-mode multicore fibers for long-haul transmission line, Opt. Fiber Technol. (2016), http://dx.doi.org/10.1016/j.yofte.2016.09.017